

## Article

# Whiterockite, $\text{CaMgMn}^{3+}_3\text{O}_2(\text{PO}_4)_2\text{CO}_3\text{F}\cdot 5\text{H}_2\text{O}$ , a new phosphate–carbonate mineral from the White Rock No.2 quarry, South Australia, Australia

Peter Elliott<sup>1,2</sup>  and Anthony R. Kampf<sup>3</sup> 

<sup>1</sup>Department of Earth Sciences, School of Physics, Chemistry and Earth Sciences, The University of Adelaide, Adelaide, SA 5005, Australia; <sup>2</sup>South Australian Museum, North Terrace, Adelaide, SA 5000, Australia; and <sup>3</sup>Mineral Sciences Department, Natural History Museum of Los Angeles County, 900 Exposition Boulevard, Los Angeles, CA 90007, USA

## Abstract

Whiterockite,  $\text{CaMgMn}^{3+}_3\text{O}_2(\text{PO}_4)_2\text{CO}_3\text{F}\cdot 5\text{H}_2\text{O}$ , is a new phosphate–carbonate mineral from the White Rock No. 2 quarry, Bimbowrie Conservation Park, South Australia, Australia. The mineral is associated with dufrénite/natrodufrénite, ushkovite, bermanite, leucophosphate and sellaite in a matrix comprising fluorapatite and minor quartz. Whiterockite has formed from hydrothermal alteration and weathering in an oxidising, low-temperature and low-pH environment. Whiterockite forms aggregates of thin platy dark-red crystals up to 0.7 mm across with individual crystals up to 0.2 mm in across. Crystals are transparent with a vitreous lustre. The mineral is brittle, has a perfect cleavage on {001} and has an irregular fracture. The measured density is  $2.76(2) \text{ g/cm}^{-3}$ . Whiterockite is optically biaxial (–), with  $\alpha = 1.660(3)$ ,  $\beta = 1.760(5)$  and  $\gamma = 1.770(5)$ , determined in white light;  $2V_{\text{meas}} = 30(1)^\circ$ ; and orientation:  $X \approx c^*$ . The mineral is pleochroic: shades of red brown;  $X < Y < Z$ . Electron microprobe analyses provided the empirical formula  $(\text{Ca}_{0.87}\text{Na}_{0.18})_{\Sigma 1.05}\text{Mg}_{1.05}(\text{Mn}^{3+}_{2.87}\text{Fe}^{3+}_{0.10})_{\Sigma 2.97}\text{O}_{1.93}(\text{PO}_4)_{2.01}\text{CO}_3\text{F}_{1.04}\cdot 4.99\text{H}_2\text{O}$ . Whiterockite is monoclinic,  $C2/m$ ,  $a = 11.112(2)$ ,  $b = 6.4551(13)$ ,  $c = 10.667(2) \text{ \AA}$ ,  $\beta = 102.61(3)^\circ$ ,  $V = 746.7(3) \text{ \AA}^3$  and  $Z = 2$ . The crystal structure of whiterockite has been refined using single-crystal synchrotron X-ray diffraction data to  $R1 = 5.10\%$  on the basis of 957 reflections with  $F_0 > 4\sigma(F_0)$ . The structure can be described as a layered structure formed by the stacking along [001] of three kinds of layers and is related to the structure of jörgkellerite.

**Keywords:** whiterockite; new mineral species; calcium magnesium manganese phosphate carbonate fluoride; pegmatite; crystal structure; White Rock No.2 quarry; Australia

(Received 27 May 2024; accepted 16 July 2024; Accepted Manuscript published online: 12 November 2024)

## Introduction

More than 70 pegmatite bodies are known to occur in the Olary Province of South Australia, many of which are rare-element pegmatites enriched in lithophile elements and characterised by abundant beryl and apatite and additional minerals such as columbite, samarskite, Nb-rutile, phlogopite and triplite-zwieselite (Lottermoser and Lu, 1997). The White Rock pegmatite and the nearby Wiperaminga Hill pegmatite were minor producers of feldspar, beryl and muscovite from the 1930s to the 1970s (Olliver and Steveson, 1982; 1984). Both are enriched in phosphate

and have yielded six new phosphate minerals between them. In the present paper we describe the new mineral whiterockite from the White Rock No. 2 quarry. The new mineral was found initially on a specimen collected from the locality in the 1960s. A visit in 2018 was able to locate several additional specimens. The mineral and name (symbol Wrc) have been approved by the International Mineralogical Association Commission on New Minerals, Nomenclature and Classification (IMA2020-044, Elliott and Kampf, 2020). The holotype specimen is housed in the mineralogical collection of the South Australian Museum, Adelaide, South Australia, Australia (registration number G34889).

## Occurrence

The White Rock pegmatite is located in the Bimbowrie Conservation Park, 24 km N of Olary, South Australia, Australia

**Corresponding author:** Peter Elliott; Email: [peter.elliott@adelaide.edu.au](mailto:peter.elliott@adelaide.edu.au)

**Associate Editor:** Daniel Atencio

**Cite this article:** Elliott P and Kampf AR (2025). Whiterockite,  $\text{CaMgMn}^{3+}_3\text{O}_2(\text{PO}_4)_2\text{CO}_3\text{F}\cdot 5\text{H}_2\text{O}$ , a new phosphate–carbonate mineral from the White Rock No.2 quarry, South Australia, Australia. *Mineralogical Magazine* 89, 127–132. <https://doi.org/10.1180/mgm.2024.66>

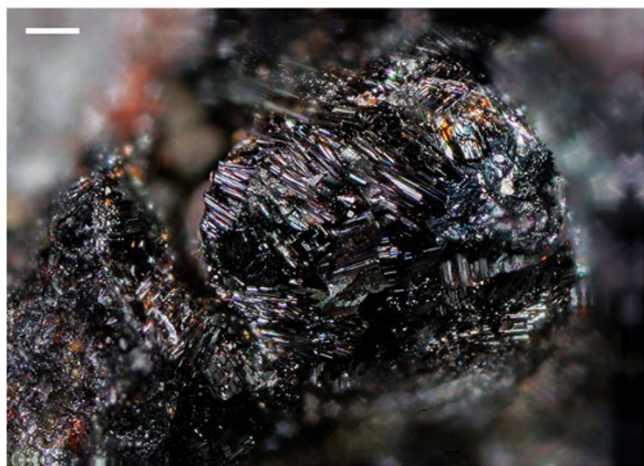


**Figure 1.** Crystal aggregate of whiterockite. The scale bar is 20  $\mu\text{m}$  in length. Holotype specimen: South Australian Museum registration number G34889.

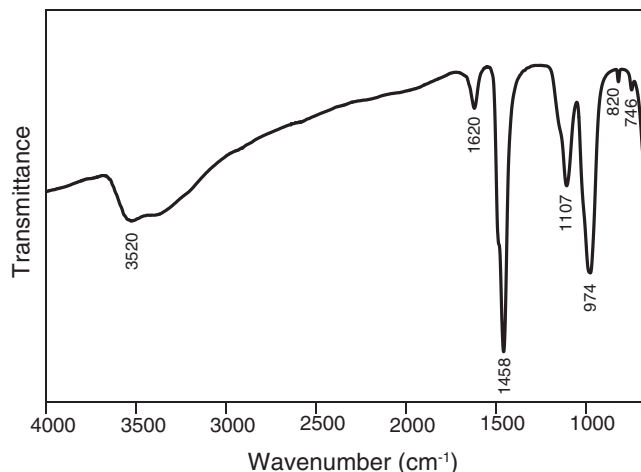


**Figure 2.** The FTIR spectrum of powdered whiterockite.

**Table 1.** Compositional data for whiterockite

Constituent	Wt.%	Range	S.D.	Probe standard
CaO	7.82	7.26–8.78	0.58	plagioclase
Na <sub>2</sub> O	0.88	0.46–1.39	0.33	albite
MgO	6.83	6.53–7.38	0.27	almandine–pyrope
Mn <sub>2</sub> O <sub>3</sub>	36.55	34.99–38.17	0.89	rhodonite
Fe <sub>2</sub> O <sub>3</sub>	1.26	0.54–2.85	0.72	almandine–pyrope
P <sub>2</sub> O <sub>5</sub>	22.95	21.66–23.96	0.78	apatite
CO <sub>2</sub> *	7.11			
F	3.17	2.90–3.67	0.26	fluorite
H <sub>2</sub> O**	14.48			
O=F	–1.33			
Total	99.72			

\*CO<sub>2</sub> calculated from the refined formula.

\*\*H<sub>2</sub>O calculated from the refined formula.

S.D. = standard deviation

(140°19'E, 32°4'S). It is a poorly outcropping beryl–columbite phosphate rare-element type pegmatite in the classification of Černý (1991). The pegmatite is hosted by rocks of the Willyama Supergroup which comprise upper greenschist to amphibolite grade metamorphosed and strongly deformed sedimentary and minor igneous rocks (Lottermoser and Lu, 1997) that are overlain unconformably by late Proterozoic Adelaidean metasediments. The pegmatite was first mined for feldspar and beryl in 1932 (Olliver and Steveson, 1982) and three quarries operated intermittently up until 1973. Recorded production is 860 tonnes of feldspar and 8.1 tonnes of beryl (Olliver and Steveson, 1984; Crooks and Abbot, 2004).

The petrogenesis of rare-element pegmatites in the Olary Block has been described in some detail by Lottermoser and Lu (1997). The pegmatites are mineralogically zoned and characterised by the occurrence of late-stage phosphate nodules between the quartz core and intermediate feldspar-rich zone. Triplite–zweieselite was formed by metasomatic alteration of magmatic fluorapatite and has been transformed by hydrothermal alteration and weathering, in an oxidising, low-temperature and low-pH environment, to give a complex, microcrystalline intergrowth of secondary phosphate minerals. At White Rock, triplite and associated secondary

phosphate minerals have been exposed in only the No.2 quarry. Secondary phosphate minerals include bermanite, bimbowrieite, cyrilovite, jahnsite-(NaFeMg), jahnsite-(NaMnMg), magnesiobermanite, mitridatite, perloffite, phosphosiderite, strunzite and ushkovite/laueite. Whiterockite is found in cavities in a matrix comprising fluorapatite and minor quartz. Associated minerals are dufrénite/natrodufrénite, ushkovite, bermanite, leucophosphite and sellaite.

### Appearance, physical and optical properties

Whiterockite occurs as aggregates of crystals up to 0.7 mm across (Fig. 1). Individual crystals are thin six-sided plates up to 0.2 mm in width with a thickness of  $\sim 1\text{--}2\ \mu\text{m}$ . Based on the crystal structure, the dominant crystal form is probably {001}. The mineral is dark red with a pink streak. The lustre is vitreous and thin crystals are transparent. The Mohs hardness is  $\sim 3$  based on scratch tests. Whiterockite is brittle with an irregular fracture and one perfect cleavage on {001}. The density measured by flotation in a mixture of methylene iodide and toluene is 2.76(2). The calculated density using the empirical formula derived from the analytical data is 2.756 g/cm<sup>3</sup>. Whiterockite is optically biaxial (–) with indices of refraction  $\alpha = 1.660(3)$ ,  $\beta = 1.760(5)$  and  $\gamma = 1.770(5)$  measured in white light. The 2V measured using extinction data analysed with EXCALIBUR (Gunter *et al.*, 2004) is 30(1)°; the calculated 2V is 33.5°. Dispersion was not observed; however, crystals provided poor conoscopic figures. The optical orientation, intuited from the structure, is  $X \approx c^*$ . Pleochroism is  $X < Y < Z$  in shades of reddish brown. The Gladstone–Dale compatibility,  $1 - (K_p/K_c)$  (Mandarino, 2007) is  $-0.052$  (good), using the empirical formula.

### Chemical data

A crystal aggregate of whiterockite was analysed using a Cameca SXFive electron microprobe operating in WDS mode with an accelerating voltage of 20 kV, beam current of 20 nA, and a 5  $\mu\text{m}$  beam diameter. Data were reduced using the  $\varphi(\rho Z)$  method of Pouchou and Pichoir (1991). Because insufficient material is available for direct determination of H<sub>2</sub>O and CO<sub>2</sub>,

**Table 2.** Powder X-ray diffraction data for whiterockite

$l_{\text{obs}}$	$d_{\text{obs}}$	$d_{\text{calc}}$	$l_{\text{calc}}$	$h\ k\ l$	$l_{\text{obs}}$	$d_{\text{obs}}$	$d_{\text{calc}}$	$l_{\text{calc}}$	$h\ k\ l$	$l_{\text{obs}}$	$d_{\text{obs}}$	$d_{\text{calc}}$	$l_{\text{calc}}$	$h\ k\ l$
100	10.385	10.4097	100	0 0 1	52	2.625	2.6534	11	$\bar{4}$ 0 2			2.0250	1	$\bar{1}$ 1 5
14	5.489	5.5467	27	1 1 0			2.6084	17	2 2 1			2.0132	2	$\bar{2}$ 2 4
		5.4220	2	2 0 0			2.6024	7	0 0 4			1.9406	1	4 0 3
83	5.247	5.3068	20	$\bar{2}$ 0 1			2.5926	2	$\bar{3}$ 1 3	35	1.741	1.7864	2	3 3 1
		5.2048	18	0 0 2	20	2.552	2.5696	14	$\bar{2}$ 2 2			1.7738	1	$\bar{4}$ 2 4
		5.1391	2	$\bar{1}$ 1 1			2.4940	8	4 0 1			1.7689	2	$\bar{6}$ 0 3
		4.6830	7	1 1 1			2.4642	4	$\bar{1}$ 1 4			1.7622	7	$\bar{2}$ 2 5
		4.0265	5	$\bar{1}$ 1 2			2.2950	1	$\bar{2}$ 2 3			1.7350	1	0 0 6
		3.6002	1	1 1 2	9	2.200	2.2262	1	$\bar{3}$ 1 4			1.7010	3	4 0 4
18	3.463	3.4699	9	0 0 3			2.1687	1	2 0 4			1.6839	1	3 3 2
		3.4020	2	2 0 2			2.1232	2	$\bar{4}$ 0 4			1.6744	1	$\bar{1}$ 3 4
4	3.239	3.1918	2	$\bar{3}$ 1 1	23	2.102	2.1106	3	1 3 0			1.6595	1	$\bar{3}$ 1 6
		3.1539	1	3 1 0			2.1044	3	$\bar{4}$ 2 1			1.6426	1	$\bar{5}$ 1 5
4	2.926	2.9586	2	$\bar{3}$ 1 2			2.1012	3	$\bar{5}$ 1 1			1.6320	2	$\bar{4}$ 0 6
		2.8704	2	3 1 1	23	2.069	2.0858	2	$\bar{1}$ 3 1			1.6272	1	5 1 3
		2.8043	1	1 1 3			2.0819	10	0 0 5	38	1.610	1.6138	6	0 4 0
		2.7754	5	$\bar{4}$ 0 1			2.0759	2	4 2 0			1.6062	1	1 3 4
46	2.760	2.7734	12	2 2 0			2.0573	3	2 2 3			1.6051	11	$\bar{6}$ 2 1
		2.7576	3	$\bar{2}$ 2 1			2.0559	2	5 1 0			1.6028	1	3 1 5
		2.7430	6	0 2 2			2.0497	1	$\bar{4}$ 2 2			1.5959	1	$\bar{6}$ 2 2
		2.7110	2	4 0 0								1.5947	1	0 4 1
		2.6700	2	2 0 3						11	1.588	1.5823	4	2 2 5

**Table 3.** Crystal data, data collection and refinement details

<b>Crystal data</b>	
Crystal dimensions ( $\mu\text{m}$ )	35 x 25 x 5
Space group	C2/m
$a, b, c$ ( $\text{\AA}$ )	11.112(2), 6.4551(13), 10.667(2)
$\beta$ ( $^\circ$ )	102.61(3)
$V$ ( $\text{\AA}^3$ ), $Z$	746.7(3), 2
$F(000)$	598.0
$\mu$ ( $\text{mm}^{-1}$ )	3.206
<b>Data collection</b>	
Diffractometer	Dectris EigerX 16M
Temperature (K)	100
Radiation	Synchrotron, $\lambda = 0.710756$ $\text{\AA}$
Crystal detector distance (mm)	108.023
Absorption correction	multi-scan, $T_{\text{min}}, T_{\text{max}} = 0.35, 0.43$
$\theta$ range ( $^\circ$ )	1.956–28.701
$h, k, l$ ranges	$-14 \rightarrow 14, -8 \rightarrow 8, -14 \rightarrow 14$
Total reflections measured	6367
Unique reflections	1039 ( $R_{\text{int}} = 0.0271$ )
<b>Refinement</b>	
Refinement on	$F^2$
$R1$ for $F_0 > 4\sigma(F_0)$	5.10%
$wR2^\dagger$ for all $F_0^2$	0.1441%
Reflections used $F_0^2 > 4\sigma(F_0^2)$	957

(Continued)

**Table 3.** (Continued.)

Number of parameters refined	94
Goof	1.122
$\Delta/\sigma_{\text{max}}$	0.000
$\Delta\rho_{\text{max}}, \Delta\rho_{\text{min}}$ ( $e^-/\text{\AA}$ )	2.246, -1.391

$$\dagger wR2 = \Sigma w(|F_o|^2 - |F_c|^2)^2 / \Sigma w|F_o|^2; w = 1/[\sigma^2(F_o^2) + (0.0787 P)^2 + 7.16 P];$$

$$P = ([\text{max of } (0 \text{ or } F_o^2)] + 2F_c^2) / 3$$

they are calculated based upon the structure determination (1 C and 19 anions pfu). Infrared spectroscopy confirmed the presence of  $\text{H}_2\text{O}$  and  $\text{CO}_3$  groups. Analytical data are given in Table 1. The empirical formula is  $(\text{Ca}_{0.87}\text{Na}_{0.18})_{\Sigma 1.05}\text{Mg}_{1.05}(\text{Mn}^{3+}_{2.87}\text{Fe}^{3+}_{0.10})_{\Sigma 2.97}\text{O}_{1.93}(\text{PO}_4)_{2.01}\text{CO}_3\text{F}_{1.04}\cdot 4.99\text{H}_2\text{O}$ . The ideal formula is  $\text{CaMgMn}^{3+}_3\text{O}_2(\text{PO}_4)_2\text{CO}_3\text{F}\cdot 5\text{H}_2\text{O}$ , which requires CaO 9.04, MgO 6.50,  $\text{Mn}_2\text{O}_3$  38.18,  $\text{P}_2\text{O}_5$  22.88,  $\text{CO}_2$  7.10, F 3.06,  $\text{H}_2\text{O}$  14.53,  $\text{O}=\text{F}$  -1.29, total 100 wt.%.

### Infrared spectroscopy

The infrared spectrum of whiterockite (Fig. 2) was obtained from a powdered sample using a Nicolet 5700 Fourier-transform infrared (FTIR) spectrometer equipped with a Nicolet Continuum IR microscope and a diamond-anvil cell. The presence of a  $\text{CO}_3$  group in whiterockite is confirmed by the presence of a strong band

**Table 4.** Fractional coordinates and displacement parameters ( $\text{\AA}^2$ ) for atoms for whiterockite

	<i>x</i>	<i>y</i>	<i>z</i>	$U_{\text{eq}}$	$U^{11}$	$U^{22}$	$U^{33}$	$U^{12}$	$U^{13}$	$U^{23}$
Ca <sup>a</sup>	0.78719(18)	1	0.72850(19)	0.0124(7)	0.0116(10)	0.0128(11)	0.0125(10)	0	0.0021(7)	0
Mg <sup>b</sup>	½	0.7599(5)	½	0.0181(10)	0.0193(16)	0.0213(17)	0.0107(14)	0	−0.0030(10)	0
Mn1	¼	¼	0	0.0158(3)	0.0172(4)	0.0138(5)	0.0185(4)	0.0055(3)	0.0085(3)	0.0060(3)
Mn2	0	0	0	0.0227(4)	0.0371(7)	0.0078(6)	0.0317(7)	0	0.0258(6)	0
P	0.38044(13)	½	0.23353(14)	0.0268(4)	0.0143(7)	0.0530(11)	0.0141(7)	0	0.0048(5)	0
C	0	½	0.000	0.0154(13)	0.013(3)	0.006(3)	0.028(4)	0	0.006(3)	0
O1	0.4117(4)	½	0.3781(4)	0.0438(16)	0.015(2)	0.099(5)	0.017(2)	0	0.0028(16)	0
O2	0.3039(3)	0.3058(5)	0.1828(3)	0.0248(7)	0.0224(14)	0.0363(17)	0.0174(12)	0.0097(12)	0.0078(10)	0.0052(13)
O3	0.5003(4)	½	0.1813(4)	0.0361(12)	0.017(2)	0.068(4)	0.026(2)	0	0.0109(17)	0
O4 <sup>c</sup>	0.0539(5)	0.3292(9)	−0.0097(5)	0.0207(17)	0.018(3)	0.013(3)	0.033(3)	0.001(2)	0.011(2)	0.000(2)
O5 <sup>d</sup>	0.1170(7)	½	0.0018(7)	0.016(2)	0.012(4)	0.013(4)	0.024(4)	0	0.003(3)	0
O6	0.1757(4)	0	0.0411(4)	0.0249(9)	0.039(2)	0.022(2)	0.0173(18)	0	0.0130(16)	0
OW7	0.6450(4)	0.7631(8)	0.4002(5)	0.0527(13)	0.033(2)	0.078(4)	0.050(2)	0.028(2)	0.0150(18)	0.016(2)
OW8/F <sup>e</sup>	0.5967(6)	1	0.6074(8)	0.0586(16)	0.060(4)	0.030(3)	0.088(5)	0	0.023(3)	0

<sup>a</sup>Refined occupancy 0.476(6); <sup>b</sup>Refined occupancy 0.641(11); <sup>c</sup>Refined occupancy 0.520(13); <sup>d</sup>Refined occupancy 0.51(2); <sup>e</sup>Refined occupancy O<sub>0.5</sub>F<sub>0.5</sub>

**Table 5.** Selected interatomic distances ( $\text{\AA}$ ) for whiterockite

Ca–OW8/F	2.226(7)	Mn2–O6	x2	1.905(5)	Mn1–O6	x2	1.907(2)	C–O4	x2	1.269
Ca–O3	2.347(5)	Mn2–O3	x2	1.933(5)	Mn1–O2	x2	1.944(3)	C–O5		1.296
Ca–O6	2.401(5)	Mn2–O4	x2	2.217(5)	Mn1–O5		2.191(5)	<C–O>		1.278
Ca–OW7	x2	<Mn2–O>		2.018	Mn1–O4		2.218(5)			
Ca–O2	x2				<Mn1–O>		2.019			
<Ca–O>	2.397	P–O1		1.505(5)						
		P–O2		1.545(4)						
Mg–OW8/F	x2	P–O2		1.545(4)						
Mg–OW7	x2	P–O3		1.553(5)						
Mg–O1	x2	<P–O>		1.537						
<Mg–O>	2.138									

**Table 6.** Bond valence analysis for whiterockite

	Ca	Mg	Mn1	Mn2	P	C	Sum
O1		0.25			1.35		1.60
O2 <sup>1</sup>	0.22 x <sup>2</sup> ↓		0.61		1.21		2.04
O2 <sup>2</sup>			0.61		1.21		1.82
O3 <sup>3</sup>	0.31			0.65	1.19		2.15
O3 <sup>4</sup>				0.65	1.19 →		1.84
O4			0.20	0.21 x <sup>2</sup> ↓		1.37 x <sup>2</sup> ↓	1.78
O5			0.23 x <sup>2</sup> →			1.29	1.75
O6 <sup>5</sup>	0.27		0.71 x <sup>2</sup> →	0.72			2.41
O6 <sup>6</sup>			0.71 x <sup>2</sup> →	0.72			2.14
OW7 <sup>7</sup>	0.27 x <sup>2</sup> ↓	0.32					0.59
OW7 <sup>8</sup>	0.27						0.27
OW7 <sup>9</sup>		0.32					0.32
OW7 <sup>10</sup>							0.00
OW8/F <sup>11</sup>	0.41	0.30					0.71
OW8/F <sup>12</sup>		0.30					0.30
Sum	1.98	1.76	3.07	3.16	4.96	4.03	

M–O bond-valence parameters are taken from Gagné and Hawthorne (2015), M–F bond-valence parameters are taken from Brown and Altermatt (1985).

Bond-valence sum for the O7 site is based on the occupancy [(H<sub>2</sub>O)<sub>0.5</sub>F<sub>0.5</sub>].

<sup>1</sup>O2 bonded to Ca, Mn1 and P; <sup>2</sup>O2 bonded to Mn1 and P; <sup>3</sup>O3 bonded to Ca, Mn2 and P; <sup>4</sup>O3 bonded to Mn2 and P; <sup>5</sup>O6 bonded to Ca, 2 x Mn1 and Mn2; <sup>6</sup>O6 bonded to 2 x Mn1 and Mn2; <sup>7</sup>OW7 bonded to Ca and Mg; <sup>8</sup>OW7 bonded to Ca; <sup>9</sup>OW7 bonded to Mg; <sup>10</sup>OW7 bonded to no cations; <sup>11</sup>OW8/F bonded to Ca and Mg; <sup>12</sup>OW8/F bonded to Mg.

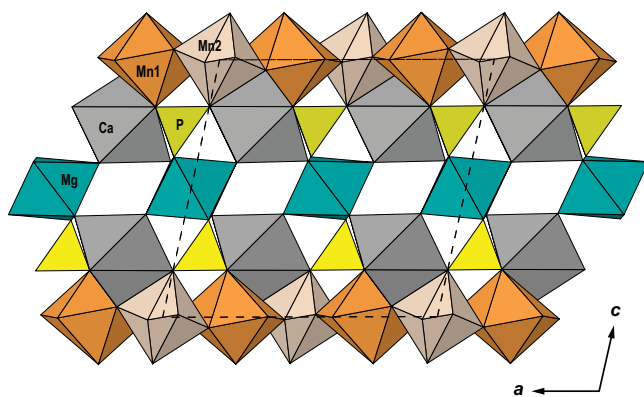


**Figure 3.** The crystal structure of whiterockite viewed along [010]. The unit cell is outlined. All structure drawings were completed using *ATOMS* (Dowty, 1999).

at  $1458\text{ cm}^{-1}$  due to the  $\nu_3$  vibration of  $\text{CO}_3^{2-}$  groups, together with the  $\nu_2$  vibration of  $\text{CO}_3^{2-}$  groups at  $820\text{ cm}^{-1}$ . The spectrum shows a broad band centred at  $3520\text{ cm}^{-1}$  that is attributed to OH stretches and a band at  $1620\text{ cm}^{-1}$  due to H–O–H bending of  $\text{H}_2\text{O}$  groups. The  $\text{PO}_4$  band occurring at  $1107\text{ cm}^{-1}$  can be assigned to the  $\nu_3$  antisymmetric stretching mode and the bands at and  $974$  and  $746\text{ cm}^{-1}$  to the  $\nu_1$  symmetric stretching mode.

### X-ray crystallography and structure determination

Powder X-ray diffraction (XRD) data for whiterockite were obtained using a Rigaku R-Axis Rapid II curved-imaging-plate microdiffractometer, with monochromatised  $\text{MoK}\alpha$  radiation ( $50\text{ kV}$  and  $40\text{ mA}$ ). A Gandolfi-like motion on the  $\varphi$  and  $\omega$  axes was used to randomise the sample. Observed  $d$  values and intensities were derived by profile fitting using *JADE Pro* software (Materials Data, Inc.). Data (in  $\text{\AA}$  for  $\text{MoK}\alpha$ ) are given in Table 2. Unit-cell parameters refined from the powder data using *JADE Pro* with whole-pattern fitting are:  $a = 11.121(10)$ ,  $b = 6.454(11)$ ,  $c = 10.601(10)\text{ \AA}$ ,  $\beta = 101.33(3)^\circ$  and  $V = 746.1(16)\text{ \AA}^3$ .

A crystal was attached to a MiTeGen polymer loop and XRD data was collected at the micro-focus macromolecular MX2 beamline at the Australian Synchrotron, part of ANSTO (Aragao *et al.*, 2018). Intensity data were collected using a Dectris EigerX 16M detector and monochromatic radiation with a wavelength of  $0.710756\text{ \AA}$ . The data was integrated in *P1* using *XDS* (Kabsch, 2010) and absorption correction was carried out with *SADABS* (Bruker, 2001). The structure was solved in space group  $C2/m$  using *SHELXT* (Sheldrick, 2015a) within the *WinGX* program suite (Farrugia, 2012) and refined using *SHELXL-2018* (Sheldrick, 2015b). The Ca and Mg sites refined to approximately half occupancy with refined occupancies of  $0.476(6)$  and  $0.641(11)$ , respectively. The refined site scattering at the Mg ( $15.3$  electrons) is greater than the value from the chemical analysis ( $12.6$  electrons) which suggests that the crystal used for single-crystal XRD may contain more Fe or Mn than that used for the chemical analyses. Two of the seven O sites, O4 and O5, associated with the  $\text{CO}_3$  group, also refined to approximately half occupancy, with refined occupancies of  $0.520(13)$  and  $0.51(2)$ , respectively. The bond-valence sum for the OW8 anion ( $0.80$  valence units, calculated using the parameters for O) lies between the values expected for donor atoms of F ( $\sim 1.0$  vu) and  $\text{H}_2\text{O}$  molecules

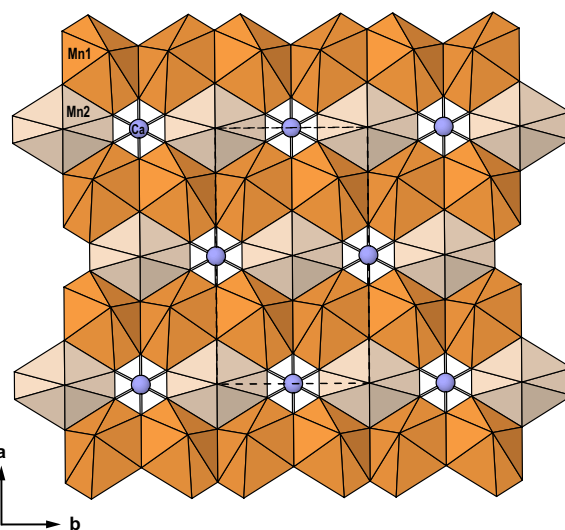


**Figure 4.** The  $[\text{Mn}_3\text{O}_8(\text{CO}_3)]$  layer in the structure of whiterockite. The unit cell is outlined.

( $\sim 0.5$  vu) indicating a mixed occupancy of the site. The chemical analysis indicates  $\sim 50\%$  occupancy of the site by F, so the site was refined with joint occupancy by O and F. The H atom locations could not be found in the difference-Fourier maps. Refinement employing anisotropic displacement parameters converged at  $R_1 = 5.10\%$  for 957 observed reflections with  $F_o > 4\sigma F_o$ . Details of the data collection and structure refinement are provided in Table 3. Fractional coordinates and anisotropic atom displacement parameters are given in Table 4, selected bond distances are reported in Table 5 and bond-valence values are given in Table 6. The crystallographic information files have been deposited with the Principal Editor of *Mineralogical Magazine* and are available as Supplementary material (see below).

### Description of the structure

The structure of whiterockite contains six cation sites. The Ca site is surrounded by seven O atoms in an augmented octahedral arrangement with a  $\langle \text{Ca-O} \rangle$  distance of  $2.397\text{ \AA}$ . The Mg, Mn1 and Mn2 sites are each surrounded by six anions in distorted octahedral coordinations.

The Mn1 and Mn2 sites exhibit four short equatorial Mn–O bonds and two long apical Mn–O bonds. Such  $[4+2]$ -distortion is typical of the Jahn–Teller distortion shown by trivalent Mn. The structure consists of three distinct layers stacked along  $[001]$  in the sequence shown in Fig. 3: (1) a layer composed of Mn octahedra and  $\text{CO}_3$  groups in which Mn1 and Mn2 octahedra share edges to form layers in which every fourth Mn site is vacant and replaced by  $\text{CO}_3$  groups (Figs 4 and 5) resulting in layers of composition  $[\text{Mn}_3\text{O}_8(\text{CO}_3)]$ ; (2) a layer formed by half-occupied Ca sites and P tetrahedra, which link by corner-sharing; and (3) a layer containing half-occupied Mg-centred octahedra. The Mn layer is flanked on either side by Ca/P layers with Ca polyhedra sharing two edges with Mn octahedra and P tetrahedra sharing corners with Mn octahedra. Two Ca layers link *via* corner-sharing Mg octahedra.

Whiterockite is structurally related to jörgellerite,  $\text{Na}_3\text{Mn}^{3+}_3(\text{PO}_4)_2(\text{CO}_3)\text{O}_2 \cdot 5\text{H}_2\text{O}$ , a layered phosphate–carbonate mineral from the Oldoinyo Lengai volcano, Gregory rift, northern Tanzania (Zaitsev *et al.*, 2017). Whiterockite is monoclinic,



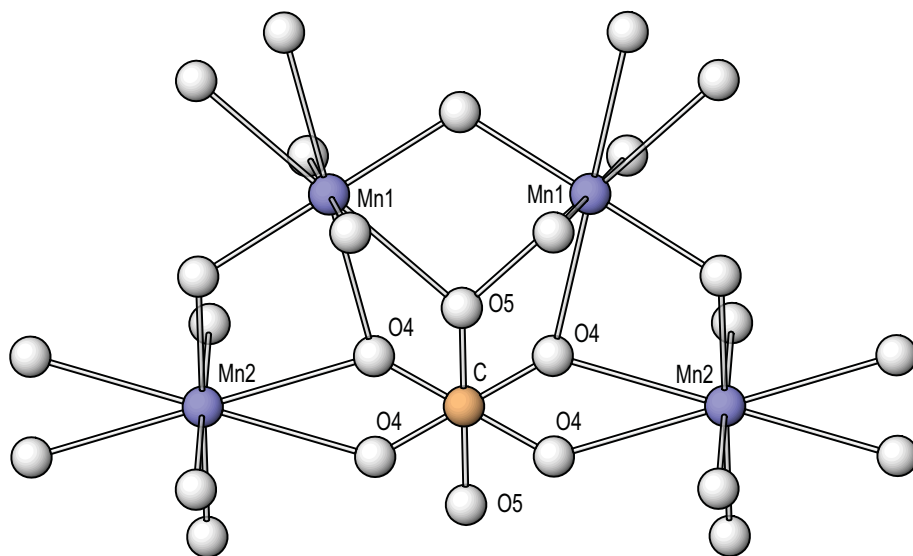


**Figure 5.** Fragment of the  $[\text{Mn}_3\text{O}_8(\text{CO}_3)]$  layer in the crystal structure of whiterockite. The O4 and O5 sites are half occupied.

whereas jörgkellerite is trigonal, space group  $P\bar{3}$  with a significantly different powder XRD pattern. Both structures consist of three distinct layers and the layer sequence in both structures is identical. Both structures contain a topologically identical  $[\text{Mn}_3\text{O}_8(\text{CO}_3)]$  layer. In jörgkellerite, this layer links to a layer comprising [7]-coordinated Na polyhedra (84% occupied) and  $\text{PO}_4$  tetrahedra, which in turn links to a layer comprising two distinct [8]-coordinated Na polyhedra (each half occupied).

**Supplementary material.** The supplementary material for this article can be found at <https://doi.org/10.1180/mgm.2024.66>.

**Acknowledgements.** The authors thank Ben Wade of Adelaide Microscopy, The University of Adelaide for assistance with the microprobe analysis. The infrared spectrum was acquired with the assistance of the Forensic Science Centre, Adelaide. This research was undertaken in part using the MX2 beamline at the Australian Synchrotron, part of ANSTO, and made use of the Australian Cancer Research Foundation (ACRF) detector. The authors thank an anonymous reviewer and Structures Editor Peter Leverett for their comments and corrections.

**Competing interests.** The authors declare none.

## References

- Aragao D., Aishima J., Cherukuvada H., Clarken R., Clift M., Cowieson N.P., Ericsson D.J., Gee C.L., Macedo S., Mudie N., Panjikar S., Price J.R., Riboldi-Tunnicliffe A., Rostan R., Williamson R. and Caradoc-Davies T.T. (2018) MX2: a high-flux undulator microfocus beamline serving both the chemical and macromolecular crystallography communities at the Australian Synchrotron. *Journal of Synchrotron Radiation*, **25**, 885–891.
- Brown I.D. and Altermatt D. (1985) Bond-valence parameters obtained from a systematic analysis of the inorganic crystal structure database. *Acta Crystallographica*, **B41**, 244–247.
- Bruker (2001) SADABS. Bruker AXS Inc., Madison, Wisconsin, USA.
- Černý P. (1991) Rare element granitic pegmatites, part I. Anatomy and internal evolution of pegmatite deposits. *Geoscience Canada*, **18**, 49–67.
- Crooks A.F. and Abbot P.J. (2004) *Beryl in South Australia*. South Australia Department of Primary Industries and Resources. Report Book, 2004/25, 15 pp.
- Dowty E. (1999) *ATOMS. Complete Program for Displaying Crystal Structures*. Version 5.0.6. Shape Software, Kingsport, Tennessee, USA.
- Elliott P. and Kampf A.R. (2020) Whiterockite, IMA 2020-044. CNMNC Newsletter No. 58; *Mineralogical Magazine*, **84**, 971–975, <https://doi.org/10.1180/mgm.2020.93>
- Farrugia L.J. (2012) WinGX and ORTEP for Windows: an update. *Journal of Applied Crystallography*, **45**, 849–854.
- Gagné O.C. and Hawthorne F.C. (2015) Comprehensive derivation of bond-valence parameters for ion pairs involving oxygen. *Acta Crystallographica*, **B71**, 562–578.
- Gunter M.E., Bandli B.R., Bloss F.D., Evans S.H., Su S.C. and Weaver R. (2004) Results from a McCrone spindle stage short course, a new version of EXCALIBUR, and how to build a spindle stage. *The Microscope*, **52**, 23–39.
- Kabsch W. (2010) XDS. *Acta Crystallographica*, **D66**, 125–132.
- Lottermoser B.G. and Lu J. (1997) Petrogenesis of rare-element pegmatites in the Olary Block, South Australia, part 1. Mineralogy and chemical evolution. *Mineralogy and Petrology*, **59**, 1–19.
- Mandarino J.A. (2007) The Gladstone-Dale compatibility of minerals and its use for selecting mineral species for further study. *The Canadian Mineralogist*, **45**, 1307–1324.
- Oliver J.G. and Steveson B.G. (1982) Pegmatites in the Olary Province. A review of feldspar and beryl mining north of Olary and the results of reconnaissance sampling of feldspar. *South Australian Department of Mines and Energy*, report 81/74.
- Oliver J.G. and Steveson B.G. (1984) Pegmatites in the Olary Province – feldspar and beryl mining. *South Australian Department of Mines and Energy, Mineral Resources Review*, **154**, 22–35.
- Pouchou J.-L. and Pichoir F. (1991) Quantitative analysis of homogeneous or stratified microvolumes applying the model “PAP”. Pp. 31–75 in: *Electron Probe Quantitation* (K.F.J. Heinrich and D.E. Newbury, editors). Plenum Press, New York.
- Sheldrick G.M. (2015a) SHELXT – Integrated space-group and crystal-structure determination. *Acta Crystallographica*, **A71**, 3–8.
- Sheldrick G.M. (2015b) Crystal structure refinement with SHELXL. *Acta Crystallographica*, **C71**, 3–8.
- Zaitsev A.N., Britvin S.N., Kearsley A., Wenzel T. and Kirk C. (2017) Jörgkellerite,  $\text{Na}_3\text{Mn}^{3+}_3(\text{PO}_4)_2(\text{CO}_3)\text{O}_2 \cdot 5\text{H}_2\text{O}$ , a new layered phosphate-carbonate mineral from the Oldoinyo Lengai volcano, Gregory rift, northern Tanzania. *Mineralogy and Petrology*, **111**, 373–381.